Exhaust Plasma Characteristics of Direct-Current Arcjet Thrusters
直流アークジェット推進機の噴出プラズマ特性

Hirokazu Tahara
Graduate School of Engineering Science, Osaka University
田原 弘一
大阪大学 大学院基礎工学研究科
1-3, Machikaneyama, Toyonaka, Osaka 560-8531, Japan
Phone:+81-6-6850-6178; Fax:+81-6-6850-6179
E-mail:tahara@me.es.osaka-u.ac.jp

Keywords: Arcjet Thruster, Space Propulsion, Exhaust Plasma

Abstract

Spectroscopic and electrostatic probe measurements were made to examine plasma characteristics with or without a metal plate for a 10-kW-class direct-current arcjet. Heat fluxes into the plate from the plasma were also evaluated with a Nickel slug and thermocouple arrangement. Ammonia and mixtures of nitrogen and hydrogen were used. The NH_3 and N_2+3H_2 plasmas in the nozzle and in the downstream plume without a plate were in thermodynamical nonequilibrium states. As a result, the H-atom electronic excitation temperature and the N_2 molecule-rotational excitation temperature intensively decreased downstream in the nozzle although the NH molecule-rotational excitation temperature did not show an axial decrease. Each temperature was kept in a small range in the plume without a plate except for the NH rotational temperature for NH_3 gas. On the other hand, as approaching the plate, the thermodynamical nonequilibrium plasma came to be a temperature-equilibrium one because the plasma flow tended to stagnate in front of the plate. The electron temperature had a small radial variation near the plate. Both the electron number density and the heat flux decreased radially outward, and an increase in H_2 mole fraction raised them at a constant radial position. In cases with NH_3 and N_2+3H_2, a large number of NH radical with a radially wide distribution was considered to cause a large amount of energy loss, i.e., frozen flow loss, for arcjet thrusters.

Introduction

The direct-current (DC) arcjet thruster is a promising device suitable for space propulsion in future missions of planetary exploration and construction of large stations. Recently, radiation-cooled arcjet thrusters were operated at input powers of 10-30 kW, and high thrust efficiencies above 30 % were achieved.

In my previous study, ammonia and mixtures of nitrogen and hydrogen, decomposing hydrazine, were used for propellants. Since these gases with large specific heats were chemically active, the thrust efficiency was enhanced at arcjet operational powers of 5-15 kW. However, plasma properties of NH_3 and mixtures of N_2 and H_2 are unknown because of complicated chemical reactions among many fragmented particle species[1-9]. Particularly, plasma characteristics near spacecraft surface are unclear because the existence of spacecraft influences the plasma characteristics[10]. It important to evaluate plasma characteristics near spacecraft because of prediction of contamination, heat load and electromagnetic interference etc.

In this study, spectroscopic and electrostatic probe measurements are made to examine plasma characteristics with or without a metal plate for a DC arcjet. Heat fluxes into the plate from plasma are also evaluated with a Nickel slug and thermocouple arrangement. Ammonia and mixtures of nitrogen and hydrogen are used. Because no other experimental data with ammonia and mixtures of nitrogen and hydrogen at the present experimental conditions are available, I make comparison with other results which used a little different condition of gas species and ambient pressure etc[11-15]. The plasma and heat flux characteristics are discussed.

Experimental Apparatus

Figure 1 shows a cross section of the DC arcjet used for this study. A constrictor of a convergent-divergent nozzle throat has a diameter of 6 mm and a length of 7 mm. A divergent nozzle has an exit diameter of 34 mm and is inclined at an angle of 52 deg. The ratio of the cross-sectional area of the nozzle exit to that of the constrictor is 32:1. As shown in Fig.1(b), the anode is provided with quartz glass rings for arc observation and optical diagnostics. A cylindrical cathode made of 2% thoriated tungsten has a diameter of 10 mm. The gap between the electrodes is set to 2 mm. Ammonia and mixtures of nitrogen and hydrogen are used. In the mixture of N_2+nH_2, the H_2 mole fraction n is varied from 0 to 3, corresponding to pure nitrogen and simulated ammonia, respectively. The gas is injected tangentially from the upstream end of the discharge chamber. The arcjet is operated with input powers of 6-12 kW. As shown in Fig.2, the arcjet is located in a vacuum tank 0.8 m in diameter and 1.5 m long, which is evacuated using a mechanical booster of 1600 l/s connected in series with a rotary pump of 160 l/s. A metal plate 100 mm x 100 mm square x 3 mm thick is also located at downstream positions from the nozzle exit. The plate position can be changed from 160 to 200 mm downstream from the arcjet nozzle exit. The plate has the ground potential.

Emission spectroscopic measurement is carried out[5-10]. The detail of the experiment including determination

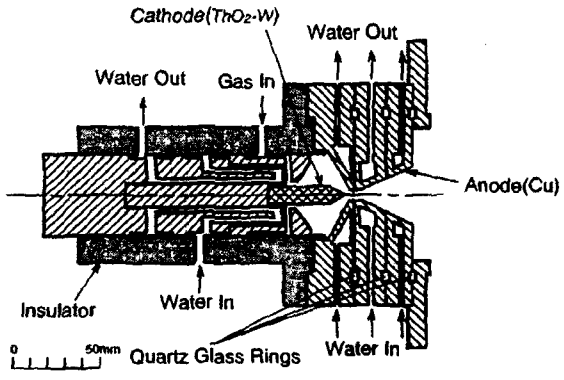

(a)

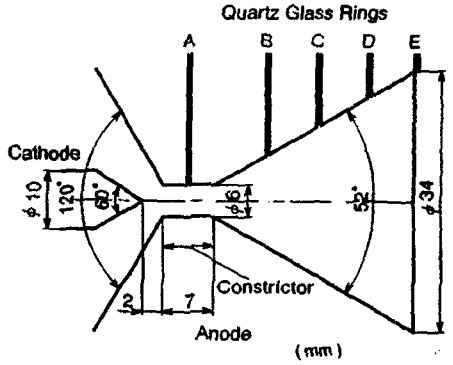

(b)

Fig.1 Cross sectional views of 10-kW-class water-cooled direct-current arcjet. (a) Configuration of DC arcjet; (b) Arrangement of electrodes and quartz glass rings.

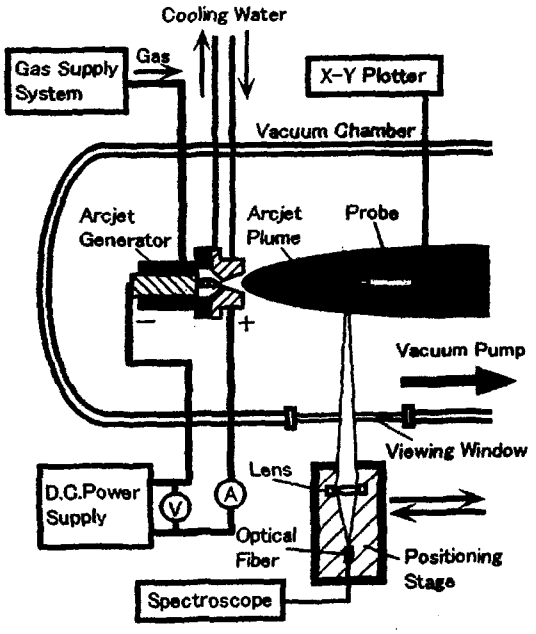

Fig.2 Experimental system of DC arcjet located in vacuum tank.

procedure of physical properties is explained in refs.5-7). The emission is collected by a lens 80 mm in focal length and is introduced into a 0.5-m monochromator through an optical fiber. The monochromator of diffraction-grating-type HAMAMATSU C5095 is provided with 150 and 2400 grooves/mm grating plates and a 1024-channel diode array detector, achieving spectral resolutions of 0.8 and 0.05 nm, respectively, per detector channel. The spectral intensities measured in this experiment are line-of-sight values, measured by looking through the arc plasma from the locations perpendicular to the central axis of the arcjet. In line-of-sight measurements, the intensity values correspond to the integrated values of intensity as a function of position. The radially dependent emission coefficient is determined from the measured spectral intensities using well-known Abel transformations.

The H-atom electronic excitation temperature is determined using a relative intensity method of spectral lines, i.e., by means of Boltzmann plotting with HI Balmer lines of 434.0, 486.1 and 656.3 nm with the assumption of local thermodynamic equilibrium (LTE). The H-atom excitation temperature is considered to be almost equal to the temperature of free electrons in plasmas with LTE conditions. The electron number density is also estimated from the Stark width of H_β line 486.1 nm. The relative intensity method cannot be used to determine the molecule-rotational excitation temperature of N_2 because the rotational lines are too close to each other. Therefore, the theoretical intensity distribution for a band is calculated with an assumed rotational temperature and compared to the measured spectrum. The transition band of N_2 $C^3\Pi_u$-$B^3\Pi_g$ at 380.4 nm (second positive band) is used. In order to simplify the calculation of radial profiles of rotational temperatures in the present study, after Abel transformations of measured emission intensities at 380.0 and 379.0 nm in the second positive band, the ratio of these intensities at a same radial position is compared to a theoretical value with an assumed rotational temperature. The molecule-vibrational excitation temperature of N_2 is determined from the relative spectral intensity method of three lower energy transitions as well as the determination of the H-atom excitation temperature. Intensive NH bands of electronic excitation $A^3\Pi$-$X^3\Sigma^-$, vibrational excitations (0-0) and (1-1) are observed. The molecule-rotational excitation temperature for the P branch band (0-0) is calculated using the relative intensity method with Boltzmann plotting of $P_{00}(10)$, $P_{00}(14)$ and $P_{00}(20)$ at 339.6, 341.0 and 343.1 nm, respectively.

Electrostatic probe measurement is also carried out in order to examine characteristics of electron temperature and electron number density on the central axis. A Langmuir probe is made of tungsten wire 0.2 mm in diameter and 5 mm long. The measurement was possible only in a far downstream plume because the probe was melted in the divergent nozzle and even near the nozzle exit. A Nickel slug 4 mm in diameter x 0.4 mm thick, the side surface of which is covered with a ceramic tube, is located on the plate surface. Heat fluxes into the plate are evaluated by measuring the temperature of the back of the slug with a K-type thermocouple, i.e., from time variations of the

temperature.

Experimental Results and Discussion

In all experiments, the discharge current and the mass flow rate are fixed to 150 A and 0.21 g/s, respectively. The input power and the tank pressure are 6.3 kW and 34 Pa for N_2, 9.45 kW and 82 Pa for N_2+H_2, 10.8 kW and 150 Pa for N_2+2H_2, 11.85 kW and 205 Pa for N_2+3H_2, and 11.7 kW and 210 Pa for NH_3, respectively.

Plasma Characteristics in Expansion Nozzle

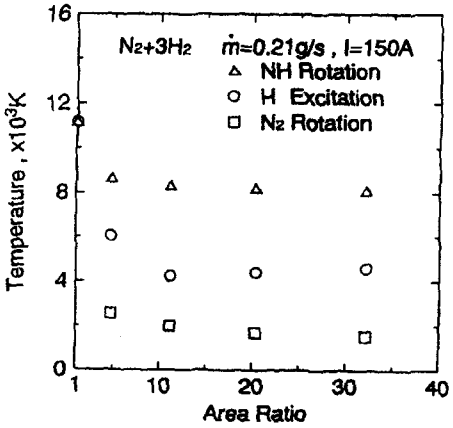

Fig.3 Axial variations in excitation temperatures of H-atom (electron), N_2 rotation and NH rotation on central axis in expansion nozzle for N_2+3H_2 gas. The area ratio is defined as the ratio of the axial-plane cross-sectional area of the expansion nozzle to that of the constrictor.

Figure 3 shows the axial variations in excitation temperatures of H atom, N_2 rotation and NH rotation on the central axis in the expansion nozzle for a mixture of N_2+3H_2 simulating ammonia. The N_2 rotational temperature in the constrictor could not be evaluated because of the noise in experiments. The H-atom electronic excitation temperature decreases from 11000 K at the constrictor to about 4000 K at a point where the area ratio is about 10, and then it keeps constant downstream. The N_2 rotational temperature also decreases downstream up to about 2000 K. On the other hand, the NH rotational temperature does not show a significant axial decrease. It is almost constant throughout the nozzle. The NH rotational temperature ranges from 8000 to 11000 K. Because the H-atom excitation temperature on the central axis in the constrictor is almost the same as the NH rotational temperature, the plasma in the constrictor is expected to be nearly in temperature-equilibrium state. However, in the expansion nozzle the plasma is in thermodynamical nonequilibrium state. Rotational temperatures of N_2 and N_2^+ only for pure nitrogen gas were observed to decrease downstream through the nozzle, as well as the N_2 rotational temperature for a mixture of N_2+3H_2 as shown in Fig.3, because of the strong coupling between the translational and rotational temperatures, i.e., because of rapid thermalization due to frequent rotational energy transfer collisions[5,6,11,12]. This behavior does not agree with that for the NH rotational temperature. This phenomenon is expected for polar molecules such as CH and NH because of rapid deexcitation before thermalization or might possibly be due to strong chemical luminescence[7]. These characteristics for the mixture gas N_2+3H_2 roughly agree with those for real ammonia NH_3. The electron number density also axially decreased on the order from 10^{16} cm^{-3} at the constrictor to 10^{14} cm^{-3} at an area ratio of 5-20[7]. I could not evaluate the electron density below 10^{14} cm^{-3} because of a narrow width of the H_β line spectrum. As a result, plasma is expected to be highly expanded, axially and radially, in the supersonic nozzle.

Plasma Characteristics in Downstream Plumes without Plates

Figure 4 shows the axial variations in excitation temperatures of H atom (presented as electron temperature), N_2 rotation, N_2 vibration and NH rotation on the central axis in the downstream plasma plume without plates for NH_3 and N_2+3H_2 gases, including electron temperatures obtained by electrostatic probe measurements. Figure 5 shows the axial variations in electron temperature and electron number density on the central axis in the downstream plume by electrostatic probe measurements. For both gases, the N_2 rotational and vibrational temperatures do not have large variations in the downstream plume, and almost stay at 1000-2000 K and at 2000-3000 K, respectively, in the plume. Although the electron temperatures intensively decrease near the nozzle, they stay at 5000-6000 K enough downstream. However, the NH rotational temperature for NH_3 decreases from 8000 to 4000 K downstream, although that for N_2+3H_2 is almost kept 8000-9000 K in the exhaust plume. This difference of the characteristics of NH rotational temperatures is explained as follows. As shown in Fig.5(b), the electron number density for N_2+3H_2 is higher than that for NH_3 because of thermal pinch effect due to rich hydrogen atoms or molecules, as predicted from plasma characteristics inside the arcjet[7,8], although the electron densities for both gases gradually decrease on the order of 10^{11}-10^{12} cm^{-3} downstream. Therefore, rotational excitations of NH molecules are considered to intensively occur in N_2+3H_2 arcs because of frequent electron collisions even in the low-pressure plume. On the other hand, the NH rotational excitations for NH_3 are relaxed because of conventional collisional energy transfer among heavy particles, i.e., thermalization.

Supersonic low-pressure nitrogen plasma jets were investigated by Robin and Domingo et al[11,12]. They measured electron temperature, electron number density and N_2^+ rotational temperature by electrostatic probe and emission spectroscopic methods. The configuration of their plasma jet generator was different from that of our plasma source, and data with ammonia and mixtures of nitrogen and hydrogen were not included; that is, only nitrogen was used. However, their vacuum tank pressure and input power were near our experimental conditions of 30-210 Pa and 9-14 kW. They showed electron temperatures around 5000 K, electron densities of 5-8x10^{13} cm^{-3} and rotational temperatures around 2500 K in an

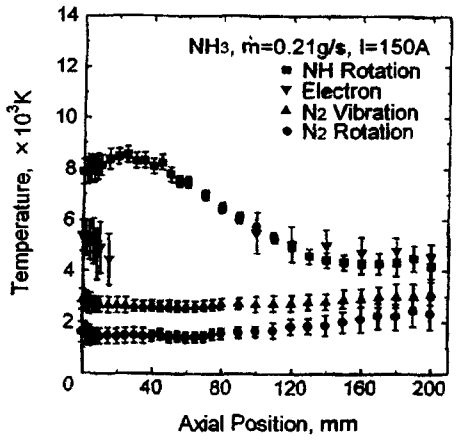

(a)

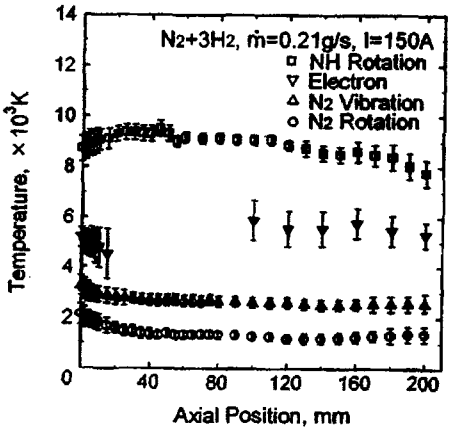

(b)

Fig.4 Axial variations in excitation temperatures of H atom (electron), N_2 rotation, N_2 vibration and NH rotation on central axis in downstream plasma plume without plates for NH_3 and N_2+$3H_2$ gases, including electron temperatures obtained by electrostatic probe measurements. In electron temperatures presented with triangle symbols, those for axial positions from zero to 20 mm correspond to H-atom electronic excitation temperatures obtained by optical measurements, and those downstream from 20 mm correspond to free-electron temperatures obtained by probe measurements. (a) NH_3; (b) N_2+$3H_2$.

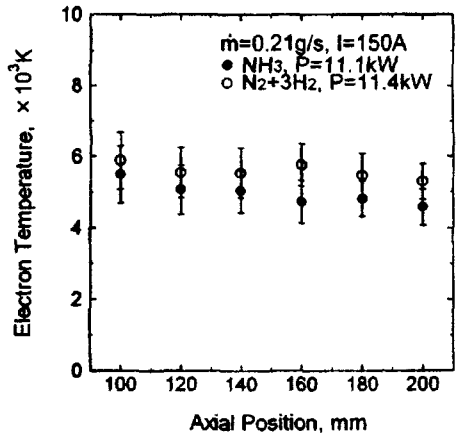

(a)

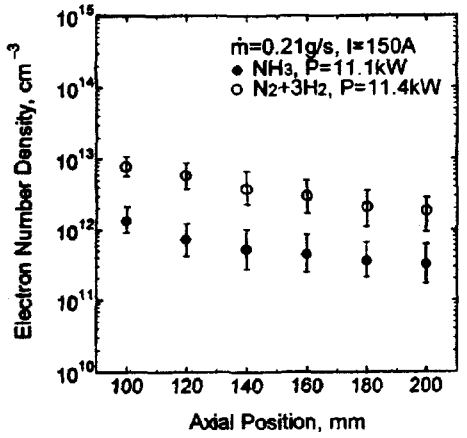

(b)

Fig.5 Axial variations in electron temperature and electron number density on central axis in downstream plasma plume without plates for NH_3 and N_2+$3H_2$ gases by electrostatic probe measurements. (a) Electron temperature; (b) Electron number density.

enough downstream region. The electron temperature and the rotational temperature roughly agree with our data with NH_3 and N_2+$3H_2$ shown in Figs.4 and 5(a), although the electron density is larger as shown in Fig.5(b).

Hidaka et al. measured electron temperature and electron number density in supersonic argon plasma flows for low-pressure plasma spraying by means of Thomson scattering of ruby-laser light[13]. The electron temperatures of 0.2-1 eV and the electron densities of the order of 10^{15} cm^{-3} were shown. Meulenbroeks et al. measured plasma parameters in expanding plasmas with mixtures of H_2 and D_2, and showed rotational temperatures below 1000 K[14]. Accordingly, although the plasma characteristics measured by other groups cannot be directly compared with our data because of different experimental conditions, large errors would not exist in our results as considering results from the different conditions.

Plasma Characteristics in Downstream Plumes with Plates

Figure 6 shows the axial variations in excitation temperatures in N_2 rotation, N_2 vibration and NH rotation on the central axis in front of the plate located at 160 mm downstream from the nozzle exit for NH_3 and N_2+$3H_2$ gases, including electron temperatures obtained by electrostatic probe measurements. Figure 7 shows the axial variations in electron temperature and electron number density on the central axis in front of the plate by electrostatic probe measurements. All temperatures in the presence of the plate for both gases almost have no variations in locations upstream from an axial position of 150 mm as well as those without plates; that is, the temperatures with the plate are almost kept constants from 120 to 150 mm. The presence of the plate does not affect the temperatures. However, in axial positions from 150 to 160 mm (up to 10 mm upstream from the plate), the plate is located at 160 mm; the

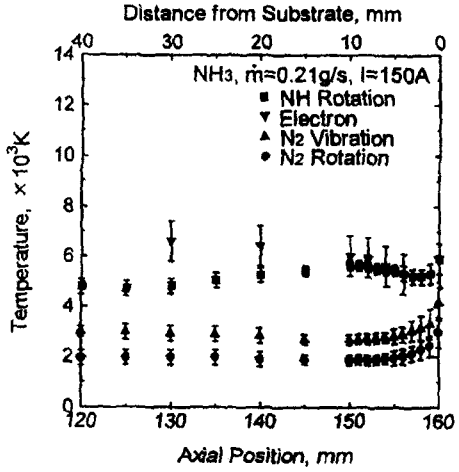

(a)

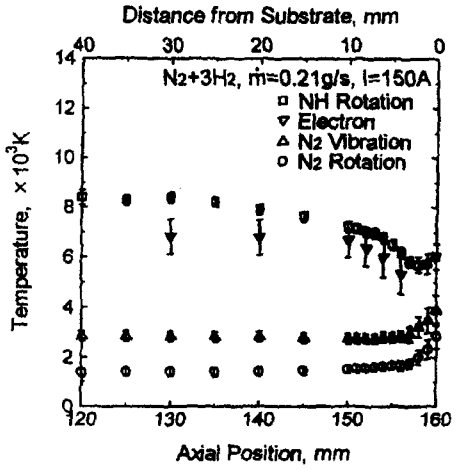

(b)

Fig.6 Axial variations in excitation temperatures of N_2 rotation, N_2 vibration and NH rotation on central axis in downstream plasma plume with plate for NH_3 and N_2+3H_2 gases, including electron temperatures obtained by electrostatic probe measurements. (a) NH_3; (b) N_2+3H_2.

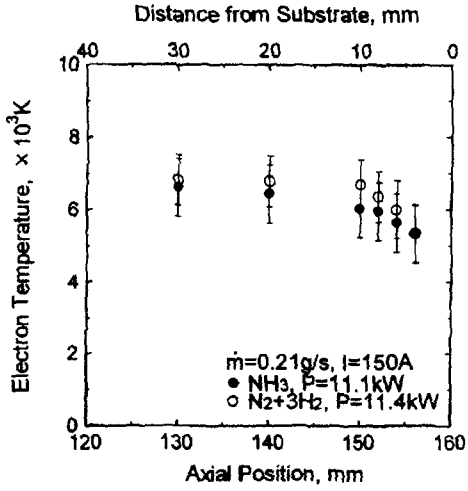

(a)

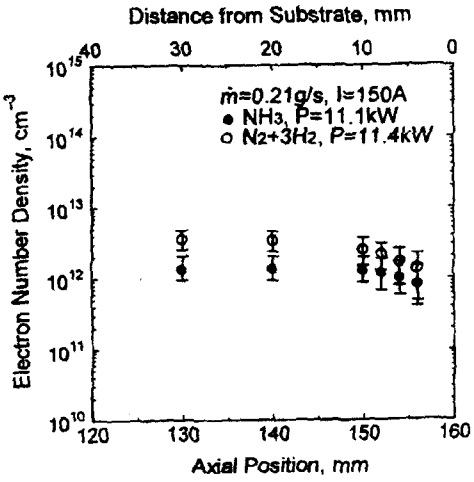

(b)

Fig.7 Axial variations in electron temperature and electron number density on central axis in downstream plasma plume with plate for NH_3 and N_2+3H_2 gases by electrostatic probe measurements. (a) Electron temperature; (b) Electron number density.

temperatures of N_2 vibration and N_2 rotation for both gases increase downstream, and the increases are by about 1000 K at the plate. On the other hand, the temperatures of NH rotation and electron gradually decrease or have small changes downstream, and then they slightly increase just in front of the plate. As a result, all temperatures are considered to approach some value around 5000 K downstream near the plate, although the surface temperature of the plate is expected to be lower. It is considered because the plate prevents plasma from flowing smoothly. In other words, since the plasma flow tends to stagnate in front of the plate, the thermodynamical nonequilibrium plasma is considered to approach a temperature-equilibrium one due to frequent energy transfer collisions among all particle species. This explanation is reasonable because the upstream stagnation temperature is roughly estimated around 4000-6000 K from the radially-average temperatures in the constrictor[7]. As shown in Fig.7(a), the electron temperature for NH_3 with the plate roughly equals that for N_2+3H_2 at a constant axial position although the electron temperature for NH_3 without the plate, as shown in Fig.5(a), is lower than that for N_2+3H_2. In the electron number density shown in Fig.7(b), the densities for both gases are almost constant in axial positions from 130 to 150 mm, and then they decrease downstream up to 157 mm. It is considered that recombination among charged particles intensively occurs just in front of the plate. The electron density for NH_3 near the plate at 157 mm is higher than that without the plate as shown in Fig.5(b), although the electron density for N_2+3H_2 with the plate is lower than that without the plate. The difference of these characteristics may be related to that of particle species between the NH_3 and N_2+3H_2 downstream plasmas[7,8].

Figure 8 shows the radial distributions of electron

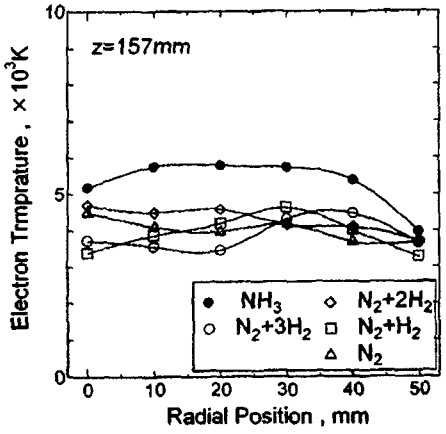

Fig.8 Radial distributions of electron temperature obtained by electrostatic probe measurements for NH_3 and mixtures of nitrogen and hydrogen with varying H_2 mole fraction at 157 mm downstream from arcjet nozzle exit in front of plate located at 160 mm.

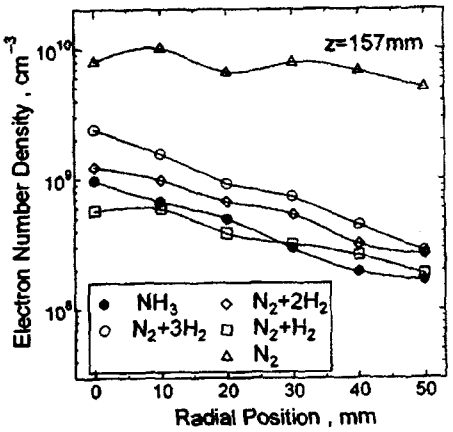

Fig.10 Radial distributions of electron number density obtained by electrostatic probe measurements for NH_3 and mixtures of nitrogen and hydrogen with varying H_2 mole fraction at 157 mm downstream from arcjet nozzle exit in front of plate located at 160 mm.

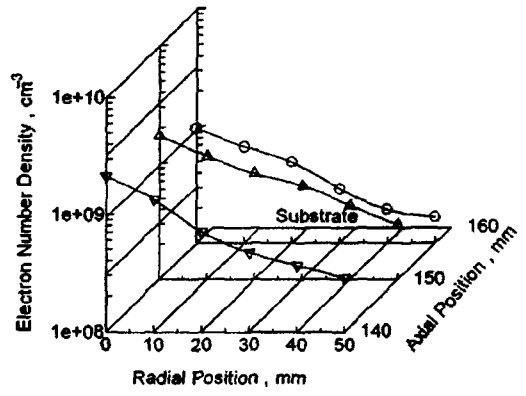

(a)

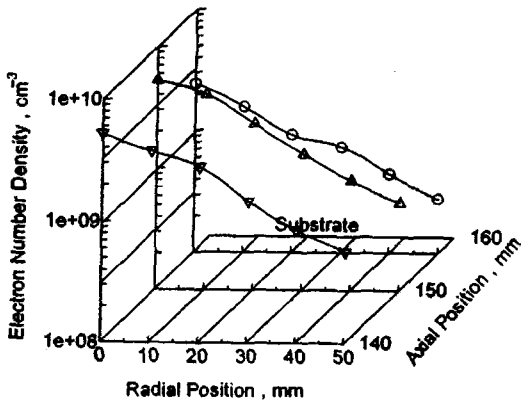

(b)

Fig.9 Radial distributions of electron number density obtained by electrostatic probe measurements for NH_3 and N_2+3H_2 gases at 140, 150 and 157 mm downstream from arcjet nozzle exit in front of plate located at 160 mm. (a) NH_3; (b) N_2+3H_2.

temperature obtained by electrostatic probe measurements for real ammonia and mixtures of nitrogen and hydrogen with varying H_2 mole fraction at 157 mm from the arcjet nozzle exit , i.e., at 3 mm upstream from the plate. The electron temperatures for all gases have small radial variations. The electron temperature for NH_3 is higher than those for pure nitrogen and mixtures of nitrogen and hydrogen at a constant radial position, and that for NH_3 is around 6000 K; those for other gases range from 3000 to 5000 K.

Figure 9 shows the radial distributions of electron number density obtained by electrostatic probe measurements for NH_3 and a mixture of N_2+3H_2 at 140, 150 and 157 mm downstream from the arcjet nozzle exit, i.e., at 20, 10 and 3 mm upstream from the plate. The electron number densities for both gases have peaks on the order of 10^9 cm^{-3} on the central axis, and they gradually decrease radially outward to the order of 10^8 cm^{-3} at 50 mm from the axis. The profile at 140 mm is almost equal to that at 150 mm. However, the electron number density at 157 mm is lower than those at 140 and 150 mm at a same radial position because of intensive recombination of electrons at 157 mm, i.e., just in front of the plate.

Figure 10 shows the radial distributions of electron number density for real ammonia and mixtures of nitrogen and hydrogen with varying H_2 mole fraction at 157 mm from the arcjet nozzle exit. The electron number density for N_2 is much higher than those for real ammonia and mixtures of nitrogen and hydrogen because the recombination hardly occurs owing to the much lower tank pressure, and because it has a small radial variation, the plasma is expected to be intensively expanded radially. On the other hand, the electron number densities for NH_3 and mixtures of N_2 and H_2 gradually decrease radially outward; an increase in H_2 mole fraction for mixture gases raises the electron number density at a constant radial position because of increasing tank pressure. The electron number density for a mixture of N_2+3H_2 simulating ammonia is higher than

that for real ammonia. This is expected because intensive recombination on heavy molecular ions of NH^+, NH_2^+ and NH_3^+ occurs near the plate with real ammonia.

Heat Flux Characteristics

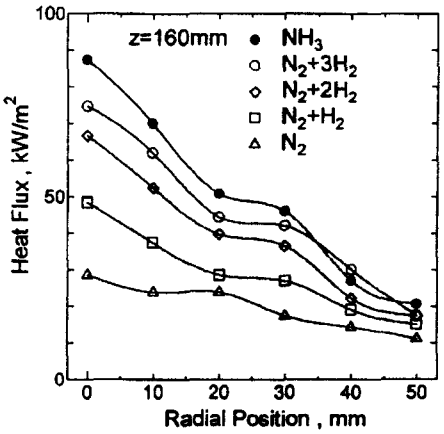

Fig.11 Radial distributions of heat flux into metal plate located at 160 mm for NH_3 and mixtures of nitrogen and hydrogen with varying H_2 mole fraction.

Figure 11 shows the radial distributions of heat flux into the plate located at 160 mm for real ammonia and mixtures of nitrogen and hydrogen with varying H_2 mole fraction. The heat fluxes for all gases decrease radially outward, and that for NH_3 is the highest at a constant radial position except at large radial positions of 40 and 50 mm; then for mixtures of N_2 and H_2 a decrease in H_2 mole fraction decreases the heat flux, although the difference in heat flux becomes small radially outward and is within 10 kW/m^2 at 50 mm. In other words, a rate of decrease in heat flux for NH_3 is the largest; then for mixtures of N_2 and H_2 the rate decreases with decreasing H_2 mole fraction. These characteristics with the plate located at 160 mm qualitatively agreed with those at 180 and 200 mm, although the heat fluxes for all gases almost linearly decreased with increasing irradiation distance because of radial expansion or diffusion of plasma with recombination.

Bolot et al. estimated heat flux by using empirical formula and numerical calculation, in which argon/hydrogen-mixture plasma jets discharging into atmospheric air and impinging on a flat plate were considered[15]. The estimated heat flux is 2-3 times larger than our data shown in Fig.11. This should be acceptable considering the differences of ambient pressure and gas species.

The heat flux into the plate is related to the plasma characteristics as mentioned above. Although the electron number density for N_2, as shown in Fig.10, is the highest at a constant radial position, the heat flux is the lowest. This is expected because the enthalpy for N_2 is the lowest owing to no H-atoms and the lowest tank pressure. Although the electron number density for NH_3 is relatively low at a constant radial position, the electron temperature, as shown in Fig.8, is the highest; the difference in temperature between NH_3 and other gases is about 1000-2000 K. Therefore, the heat flux for NH_3 is expected to be the highest because of the high enthalpy by a large amount of high-temperature H-atoms and the highest tank pressure.

When a titanium plate was used, nitriding of the plate surface occurred by exposure to the plasma jet. In the nitriding experiments, in cases with NH_3 and a mixture of N_2+3H_2, hard TiN-rich surfaces were made even at a large radial position of 50 mm[3,4]. Because the heat fluxes for NH_3 and a mixture of N_2+3H_2 are almost equal to those for other gases at 50 mm, all surface temperatures are almost the same. As a result, the better nitriding characteristics cannot be explained with the difference in surface temperature. Although the detailed physical phenomena are not clear, a neutral radical of NH with a radially wide distribution, as predicted from Figs.6 and 8, is considered to contribute to the nitriding as a chemically active and non heating process. Therefore, a large number of NH radical was considered to cause a large amount of energy loss, i.e., frozen flow loss, for arcjet thrusters.

Conclusions

Spectroscopic and electrostatic probe measurements were made to examine plasma characteristics with or without a metal plate for a DC arcjet. Heat fluxes into the plate from plasma were also evaluated with a Nickel slug and thermocouple arrangement. Ammonia and mixtures of nitrogen and hydrogen were used. In the mixture of N_2+nH_2, the H_2 mole fraction n was varied from 0 to 3, corresponding to pure nitrogen and simulated ammonia, respectively. The NH_3 and N_2+3H_2 plasmas in the nozzle and in the downstream plume without a plate were in thermodynamical nonequilibrium states because the electron number densities rapidly decreased downstream, although they were nearly in temperature-equilibrium at the constrictor throat. As a result, the H-atom electronic excitation temperature and the N_2 molecule-rotational excitation temperature intensively decreased from 11000 K at the constrictor to 4000 K and to 2000 K at the nozzle exit, respectively, with a mass flow rate of 0.21 g/s and an electric input power of about 11 kW although the NH molecule-rotational excitation temperature did not show an axial decrease. Each temperature was kept in a small range in the plume without a plate except for the NH rotational temperature for NH_3 gas. On the other hand, as approaching the plate, the thermodynamical nonequilibrium plasma came to be a temperature-equilibrium one because the plasma flow tended to stagnate just in front of the plate. The electron temperature had a small radial variation near the plate. Both the electron number density and the heat flux decreased radially outward except for the electron density for N_2, and an increase in H_2 mole fraction raised them at a constant radial position because of increasing tank pressure. Although the electron number density for N_2 was the highest at a constant radial position, the heat flux was the lowest. This is expected because the enthalpy for N_2 is the lowest owing to no H-atoms and the lowest tank pressure. Although the electron number density for NH_3 was relatively low, the electron temperature was the highest.

Therefore, the heat flux for NH_3 is expected to be the highest because of the high enthalpy by a large amount of high-temperature H-atoms and the highest tank pressure. In cases with NH_3 and N_2+3H_2, a large number of NH radical with a radially wide distribution was considered to cause a large amount of energy loss, i.e., frozen flow loss, for arcjet thrusters.

References

1) F. Gitzhofer, K. Mailhot, M.I. Boulos, I.H. Jung, J.S. Lee and H.S. Park," Fabrication of Simulated Nuclear Fuel Pellets by Induction Plasma Deposition," Proceedings of the 15th International Thermal Spray Conference, Nice, France, 2(1998), pp.1283-1288.

2) K. Mailhot, F. Gitzhofer and M.I. Boulos," Supersonic Induction Plasma Spraying of Yttria Stabilized Zirconia Films," Proceedings of the 15th International Thermal Spray Conference, Nice, France, 2(1998), pp.1419-1424.

3) H. Tahara, H. Yoshikawa, Y. Andoh, T. Yasui, K. Onoe and T. Yoshikawa," Surface Nitriding of Titanium Using Low Pressure Nitrogen Plasma Jet," Proceedings of the International Symposium on Designing, Processing and Properties of Advanced Engineering Materials, Toyohashi, Japan, 1997, pp.523-528.

4) Y. Andoh, S. Tobe, H. Tahara and T. Yoshikawa," Nitriding of Titanium Plate and Atmospheric Plasma Sprayed Titanium Coating Using Nitrogen Plasma Jets under a Low Pressure Environment," Proceedings of the United Thermal Spray Conference, Dusseldorf, Germany, 1999, pp.234-239.

5) H. Tahara, N. Uda, K. Onoe, Y. Tsubakishita and T. Yoshikawa," Discharge Features in a Steady-State Nitrogen Arcjet Engine with an Expansion Nozzle," IEEE Trans. Plasma Sci., 22(1994), pp.58-64.

6) H. Tahara, K. Komiko, T. Yonezawa, Y. Andoh and T. Yoshikawa," Thermodynamical Nonequilibrium Nitrogen Plasmas in a Direct-Current Arcjet Engine Nozzle," IEEE Trans. Plasma Sci., 24(1996), pp.218-225.

7) H. Tahara, T. Yonezawa, Y. Andoh and T. Yoshikawa," Emission Spectroscopic Measurement of Ammonia or Mixture of Nitrogen and Hydrogen Plasma in a Direct-Current Arc Jet Generator with an Expansion Nozzle," IEEE Trans. Plasma Sci., 26(1998), pp.1307-1313.

8) H. Tahara, T. Shibata, Y. Andoh, T. Yasui, K. Onoe and T. Yoshikawa," Plasma Characteristics of Supersonic Ammonia and Nitrogen/Hydrogen-Mixture Plasma Jets under a Low Pressure Environment," Proceedings of the United Thermal Spray Conference, Dusseldorf, Germany, 1999, pp.720-725.

9) H. Tahara, T. Shibata, Y. Ando, K. Onoe and T. Yoshikawa," Exhaust Plume Characteristics of a Supersonic Ammonia or Nitrogen/Hydrogen-Mixture Plasma Jet Generator under a Low Pressure Environment," Proceedings of the 14th International Symposium on Plasma Chemistry, Prague, Czech Republic, 2(1999), pp.563-568.

10) H. Tahara, T. Shibata, K. Mitsuo and T. Yoshikawa," Diagnostic Measurement of Supersonic Ammonia and Nitrogen/Hydrogen-Mixture DC Plasma Jets for Nitriding under a Low Pressure Environment," Proceedings of the 1st International Thermal Spray Conference, Montreal, Canada, 2000, pp.21-28.

11) L. Robin, P. Vervisch and B.G. Cheron," Experimental Study of a Supersonic Low-Pressure Nitrogen Plasma Jet," Phys. Plasmas, 1(1994), pp.444-458.

12) P. Domingo, A. Bourdon and P. Vervisch," Study of a Low Pressure Nitrogen Plasma Jet," Phys. Plasmas, 2(1995), pp.2853-1862.

13) R. Hidaka, T. Ooki, K. Takeda, K. Kondo, H. Kanda, K. Uchino, Y. Matsuda, K. Muraoka and M. Akazaki," Ruby-Laser Scattering Diagnostics of a Supersonic Plasma Flow for Low-Pressure Plasma Spraying," Jpn. J. Appl. Phys., 26(1987), pp.L1724-L1726.

14) R.F.G. Meulenbroeks, D.C. Schram, M.C.M. van de Sanden and J.A.M. van der Mullen," Wall Association and Recirculation in Expanding Thermal Arc Plasmas," Phys. Rev. Lett., 76(1996), pp.1840-1843.

15) R. Bolot, C. Coddet, M. Imbert and V. Monin," Mathematical Modeling of a Plasma Jet Impinging on a Flat Structure," Proceedings of the 15th International Thermal Spray Conference, Nice, France, 1998, pp.439-444.